Composite Structures 319 (2023) 117149

Contents lists available at ScienceDirect

Composite Structures

journal homepage: www.elsevier.com/locate/compstruct

Sound insulation performance of honeycomb core aluminum sandwich panels with flexible epoxy-based foam infill

Yalçın Boztoprak [a], Merve Ünal [b], Çağatay Özada [b], Eslem Kuzu [b], Hakkı Özer [b], Furkan Ergin [b], Murat Yazıcı [b,*]

[a] Marmara University, Technology Faculty, Metallurgical and Materials Eng. Department, İstanbul, Turkey
[b] Applied Mechanics and Advanced Materials Research Group (AMAMRG) Lab., Automotive Eng., Eng. Faculty, Bursa Uludağ University, Bursa, Turkey

ARTICLE INFO

Keywords:
Acoustic properties
Sound insulation
Foam filling
Sandwich panel
Honeycomb core
Flexible epoxy

ABSTRACT

The most distinctive features of sound insulation structures are their flexibility and porosity. Therefore, the flexible epoxy matrix material was made cellular using a suitable foaming agent. In addition, hollow glass microspheres (HGMs) were added to the epoxy matrix. Thus, the sound wave refraction was increased by obtaining cavities in the cell walls. Structures with different densities and voids were created by changing the ratios of the filling material and foaming agents used in the sandwich. An aluminum (Al) honeycomb was used to protect the insulation materials' structural integrity and ensure the homogeneous distribution of sound waves. The effect of density differences on sound insulation values was investigated. The mechanical properties of sandwich structures were determined using compression and three-point bending tests. The distribution of the filler in the matrix was visualized using SEM. TGA, DSC, thermal conductivity, dielectric, and flammability tests were also performed to determine their thermal, electrical, and flammability properties. During the formation of cells in the flexible epoxy, the HGMs were positioned in the cell wall by internal gas pressure. Low-density structures performed better at low frequencies, while high-density structures at high frequencies.

1. Introduction

As with rapid urbanization and transportation development, noise pollution has also been a significant issue, leading to various health risks such as tinnitus, sleep disturbance, and even ischemic heart disease [1]. For this reason, it is important to control the noise coming from the living environment [2]. Removing damage using sound-absorbing materials is an effective way to solve these problems [3]. However, conventional sound-absorbing materials have the disadvantage that sounds absorption remains in the narrow frequency band [4,5]. For this reason, a study is being done on producing a wide-band porous sound absorber known as smart hybrid foam, a hybrid active–passive sound-absorbing material [6]. These hybrid foam structures, which can withstand high compressive stresses, deformation, and damage tolerance [12], perform damping in a wide frequency range [7].

Sound-absorbing foam materials consist of channels, cracks, or voids that allow sound waves to enter the materials. The energy fields that pass through the porous structure of these sound absorption materials are effectively dispersed or blocked due to their complex structure. In these materials, thermal loss occurs due to the friction of air molecules with the pore walls. In addition, viscous losses occur in the materials caused by the airflow [1]. These losses reduced the sound energy. These energy consumption principles are found in porous materials with wide frequency bands for sound absorption [8,9]. In some studies [10–12], they have produced various sound-absorbing thermoplastic polymer foams. These thermoplastic foams with acoustic performance have insufficient strength and heat stability [13]. The thermoset polymer commonly used in foam production is polyurethane foams. Polyurethane foams used for sound insulation are disadvantageous because they cannot provide good sound insulation in low-frequency situations [14,15]. Epoxy foams, utilized as an alternative to polyurethane foam, are the best choices for structural applications compared to other thermoset foams [13] because of their high strength characteristics. However, the stiffness of structural epoxy foams is very high. In structural applications, epoxy foam's rigidity diminishes the intended elastic energy absorption capacity. Therefore, sound insulation foams can be developed by adding flexible molecules to epoxy resin chain groups. On the other hand, studies have been carried out to evaluate different sound

* Corresponding author.
E-mail address: myazici@uludag.edu.tr (M. Yazıcı).

https://doi.org/10.1016/j.compstruct.2023.117149
Received 1 January 2023; Received in revised form 27 March 2023; Accepted 11 May 2023
Available online 20 May 2023

absorption mechanisms and to syntactic foam with various functional properties by adding HGMs to epoxy resins [16–18].

In the study of Gao et al. [19], a syntactic foam structure was formed with epoxy resin and HGMs. The effect of the prepared syntactic structure on sound absorption and sound transmission loss properties was investigated. Therefore, it was found that adding HGMs effectively reduced the specific acoustic impedance of the epoxy resin matrix. Syntactic foam materials have many properties, such as low density, high specific strength, superior sound and heat insulation, and energy absorption during impact [20–22]. Furthermore, syntactic foam systems developed according to usage areas are exposed to strength and force couples of different axes. For this reason, syntactic foams are developed in sandwich structures, and their structural stability is increased. In addition, these developed structures can contribute to sound absorption performance by separating sound waves [23–27].

Sandwich structures offer sound and vibration damping, thermal insulation, superior bending stiffness, and high energy absorption upon impact [28–32]. Honeycombs are one of the most common sandwich cores. The honeycomb core has a regular hexagonal structure distinguished by its cell size, material, cell wall thickness, and bulk density. Many studies have been in the literature about sound transmission loss and sound insulation of sandwich structures [33–36]. In this regard, it is intended to raise the structural stability of syntactic sound-absorbing foams by incorporating them into Al honeycomb sandwich core cells and improve the sound absorption and transmission capabilities of sound waves by dividing them into several cells.

In this study, a sandwich panel with sound absorption and low sound transmission properties was developed. A hexagonal honeycomb Al structure was used as a sandwich panel core. Using flexible and cellular materials in sound absorption structures influences the sound waves' diffraction and absorption. Due to this, the matrix material was selected as flexible epoxy. Furthermore, as an inorganic chemical foaming agent, sodium bicarbonate ($NaHCO_3$) was preferred to produce cellular morphology in flexible epoxy.

Additionally, HGMs were incorporated into the flexible epoxy matrix before foaming. During the foaming of the resin mixture (Flexible epoxy resin + hardener + HGMs), the large closed cells were created by the foaming agent, and HGMs were also positioned in these cell walls due to the pressure of gases produced inside the large cells. Thus, the objective was to develop a novel syntactic foam to achieve low density and superior sound absorption characteristics. The sound absorption and sound transmission properties of the developed hybrid sandwich panels were examined by an impedance tube. The correlation between epoxy foams' density, sound absorption, and sound transmission properties was evaluated according to the results. The low-density syntactic foam was observed to have superior sound absorption properties at low frequencies and high-density foam at high frequencies. The distribution of porous structures in the matrix was analyzed by scanning electron microscopy (SEM). Compression and three-point bending tests were performed to determine the structure's strength and stiffness. Thermal gravimetric analysis (TGA), differential scanning calorimetry (DSC), thermal conductivity, dielectric, and flammability tests were carried out to determine the thermal and electrical characterization.

2. Materials and methods

2.1. Materials

In this study, a porous and flexible structure was developed. SLW 0179 coded flexible epoxy resin (CET Composite and Epoxy Technologies Corp., Turkey) was used as a matrix material in sound insulation structures. Sodium bicarbonate ($NaHCO_3$) (Tekkim Chemical, Turkey) was used as a foaming agent to make the matrix material cellular. Hollow glass microspheres (K15, d = 0.15 g/cc, 60 μm diameter, 3 M Company) as the filling material were incorporated into the matrix material. The aluminum honeycombs (Al 3005-H19) with a sandwich height of 20 mm, a cell size of 6.78 mm, and a foil thickness (50 μm) were used. (Altıgen Aerospace Panel Limited Company, Turkey). In addition, aluminum top and bottom face sheets (Al 5754-H22) with a thickness of 1 mm were used.

2.2. Preparation of sandwich specimens

Before the foaming process, the matrix material was mixed with a foaming agent ($NaHCO_3$) and HGMs. The resultant mixture was injected into the Al honeycomb cells. Then, sandwich constructions were manufactured by bonding Al sheets to the top and bottom faces of the honeycomb core. (Fig. 1).

The dimensions of 50 × 200x20 mm and 50 × 50x20 mm specimens were prepared for three-point bending and compression tests, respectively. Cylindrical specimens with 30 mm and 100 mm diameters were also prepared for sound insulation tests. A 1 mm thick Al sheet was used for the specimens' top and bottom faces. An Epoxy (G-Flex) adhesive was used to hold these plates together. To ensure adhesion, it was cured for 60 min at 70 °C.

2.3. Production of hybrid cell epoxy syntactic foam

Sodium bicarbonate ($NaHCO_3$), due to the volume of carbon dioxide released during decomposition and the fact that it decomposes at a relatively low temperature, frequently produces an cell structure suitable for use with polymer. Therefore, NaHCO3 and HGMs were added in specific proportions into the flexible epoxy resin to produce epoxy foam. For 10 min, this mixture was stirred with a mechanical mixer. Although the decomposition of the $NaHCO_3$ starts at 38 °C and the optimum temperature range is 121 to 149 [37], above 127 °C, this decomposition is very rapid [38]. Considering this situation, a preheating process (140 °C) was applied to the Al honeycomb, and the obtained mixture was filled into preheated Al honeycomb cells. Then this specimen was kept in the oven for 30 min at a fixed 140 °C temperature. As mentioned above, $NaHCO_3$ exposed to a temperature above 127 °C decomposes, creating a rapid gas formation with the CO_2 gas and H_2O vapor formed (Fig. 2).

2.4. Sound insulation and transmission

Porous sound insulation materials are structures where sound waves are broken and weakened. These materials attract attention as the ideal material for noise control in many sectors, such as automotive and transportation. Fig. 3 schematically shows an impedance tube setup with a specimen. The sound absorption coefficient shows how much sound insulation materials absorb sound. This coefficient varies according to density, elasticity, thickness, and flow resistance. In addition, the sound absorption coefficient at the vertical incidence angle is determined by the impedance tube [39] and calculated analytically [40].

The sound absorption coefficient in impedance tubes is determined

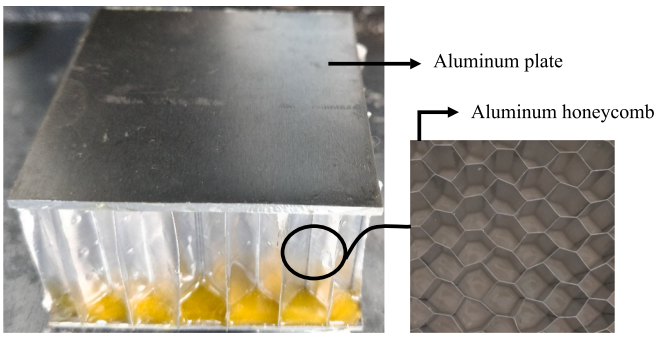

Fig. 1. Aluminum Honeycomb and Sandwich Structure.

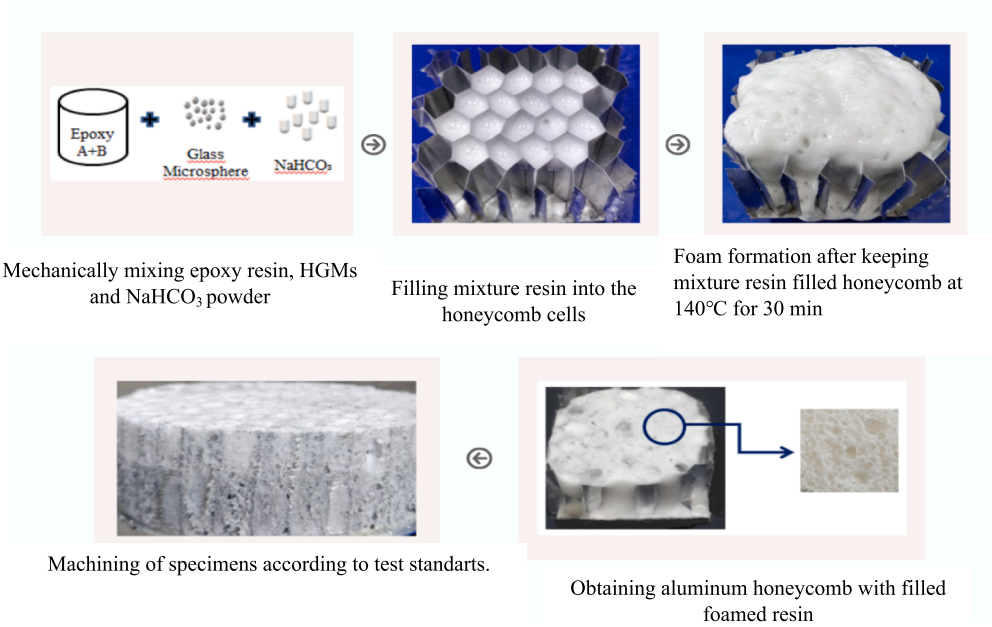

Fig. 2. Production Scheme of Epoxy Syntactic Foams.

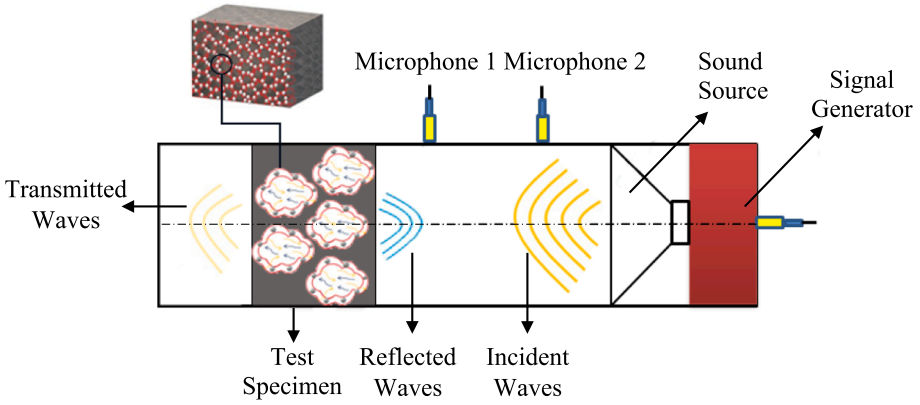

Fig. 3. Schematic Diagram of Impedance Tube.

by frequency response functions (FRF) measured by microphones placed in different axial positions. It is crucial to determine the internal swallow of the tube in order to make accurate measurements in this method. The ASTM E1050-12 standard empirically determines the internal absorption of the tube. The following theoretical calculations were used for sound performance measurements [41]. The data measured in the impedance tube was the sound power, and the sound transmission loss (TL) value was calculated using Equation (1).

$$TL = 10\log_{10}\left(\frac{W_{src}}{W_{rec}}\right) \tag{1}$$

Equations (2) and (3) were used to calculate the sound absorption coefficients.

$$\alpha = 1 - |R|^2 = 1 - R_r^2 - R_i^2 \tag{2}$$

$$R = |R| \cdot e^{j\varphi R} = R_\Gamma + jR_i$$

Normal specific acoustic impedance ratio

$$\frac{z}{\rho c} = \frac{r}{\rho c} + \frac{jx}{\rho c} = \frac{1+R}{1-R} \tag{3}$$

and ρ is air density (g/cm^3) which is calculated as

$$\rho = 1.290\left(\frac{P}{101.325}\right)\left(\frac{273.15}{273.15+T}\right) \tag{4}$$

where P is atmospheric pressure (kPa) and T is the room temperature (°C).

Estimation of 1/3 octave and 1/1 octave results:

$$\alpha_{band} = \frac{1}{n}\sum_{i=1}^{n}\alpha_{f_i} \tag{5}$$

Where, α_{band} is the absorption coefficient of the desired 1/3 octave or 1/1 octave band, n is the number of bins in the band,f_i is frequency bin in the desired 1/3 octave or 1/1 octave to be estimated and α_{f_i} is the absorption measured by this test method in the indicated frequency bin.

All measurements were performed by using a Testsens® impedance tube (Bias Co/Turkey). Experiments were performed according to ASTM 1050–1 [39].

In an impedance tube measurement, the tube diameter determines the upper limit of the frequency range of sound waves in which safe measurements are made. Aluminum honeycomb sandwich specimens

with thicknesses of 20 mm, 30 mm, and 100 mm were produced for this study. As a result, these samples' sound transmission loss and sound transmission coefficients of these specimens were obtained.

2.5. Mechanical tests

Tensile properties of the manufactured foam were performed at 5 mm/min crosshead speed in a Zwick Proline Z010 TH Universal Tensile-Compression test machine using proper grips. The specimens were produced following the ASTM D638-14 standard.

Compression tests were performed for the pure flexible epoxy material, the developed hybrid epoxy syntactic foam, and sandwich panels. These tests were conducted in accordance with ASTM 365. The loading capacity of the Zwick Proline Z010 TH compression testing machine is 10 kN. For each specimen, the crosshead speed was 5 mm/min.

Three-point bending tests were performed using the UTEST-7014 Universal tensile/compression machine, shown in Fig. 4a, under 5 mm/min crosshead speed according to ASTM C480 standard. The test fixture and essential dimension are shown in Fig. 4b. Thus, the material's toughness, displacement during deformation, and bending strength values were determined.

2.6. Material characterizations

A scanning electron microscope (SEM, ZEISS EVO40) was used at an acceleration voltage of 20 kV to determine pore morphologies. SEM images with 100x, 500x, and 2000x magnifications were taken from the specimen and evaluated.

Thermogravimetric analysis (TGA) experiments were performed on the TA/SDT650 device. Specimens with a 5 ± 0.5 mg mass were increasingly heated from 40 to 600 °C at 10 °C/min under nitrogen flow (80 ml/min). Differential Scanning Calorimetry (DSC) measurements of 4 ± 0.5 mg specimen were performed with TA/Discovery DSC250 instrument under nitrogen flow.

The epoxy foams' thermal conductivity (κ) was made and evaluated in C-Therm/TCI brand device according to ISO 8302:1991 standard. Three specimens measuring 300 × 300 × 25 mm were measured, and the average value was recorded.

The dielectric property of the 2 mm thick and 1.5 cm wide specimen produced was measured according to the ASTM D-150 standard. This test was carried out on Novotherm-HT 1200 Model device at room temperature and 0–100 kHz frequency.

The flammability test was performed on UL94 flammability test equipment-ATLAS in accordance with the UL 94 HBF standard for sound insulation foam materials.

3. Results and discussion

3.1. Morphology of cell and foaming process

Fig. 5a shows large cells and homogeneously dispersed HGMs on the cell walls. Large cells were obtained due to the reaction of $NaHCO_3$ added to the flexible epoxy matrix with heat. In Fig. 5b and Fig. 5c, the presence of HGMs inside the walls of the elastic matrix is seen. Closed large and closed microcells were used together in the study. The foaming agents produced large cells, and microcells were included directly with HGMs. Thus, the objective is to weaken sound waves by dividing them into large cells and confining the weak waves in rigid HGMs.

Specimens of 5 different densities produced in this study are shown in Table 1. These specimens were obtained by varying the ratios of flexible epoxy, $NaHCO_3$, and HGMs. The proportion of closed cells also increases as the percentage by weight of HGM in the structure increases. Increasing the closed-cell ratios contributes to the refraction of sound waves. For this reason, the glass sphere ratio should be at maximum levels. The rate of HGMs added varies according to the matrix material and the viscosity of the material. The addition of HGMs increases the viscosity of the matrix. Although the literature reports rates of up to 20% of the weight of the HGMs [19], these rates cannot be achieved because the flexible epoxy, which has an elastic structure, is much more viscous. Furthermore, it was shown in another study that adding more than 10% HGMs reduced sound transmission loss [24]. For this reason, the rate of HGMs in the matrix was set at 10%.

It is known that $NaHCO_3$ compounds can react with weak acids to produce carbon dioxide gas. It is also important to remember that acids can react with epoxy groups [42–45]. However, $NaHCO_3$ can also decompose with an increase in temperature. It can produce carbon dioxide, water, and sodium carbonate. The residue resulting from the reaction is harmless as a chemical filler. However, in this study, in which

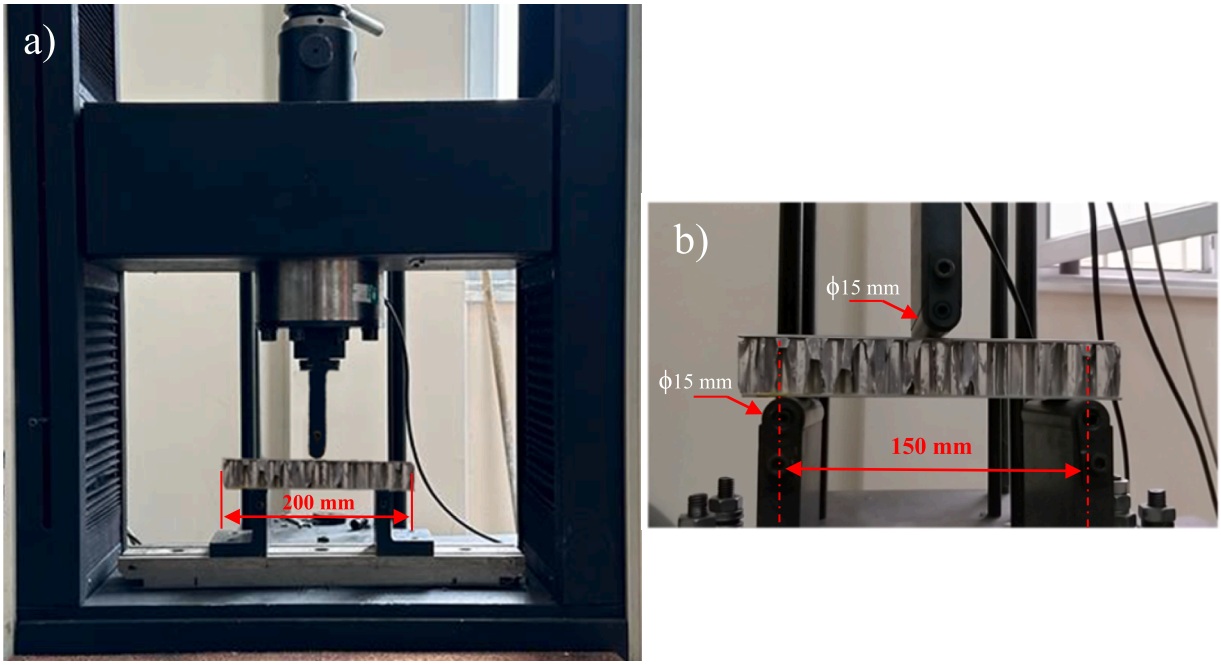

Fig. 4. 3-point bending test fixture and essential dimensions.

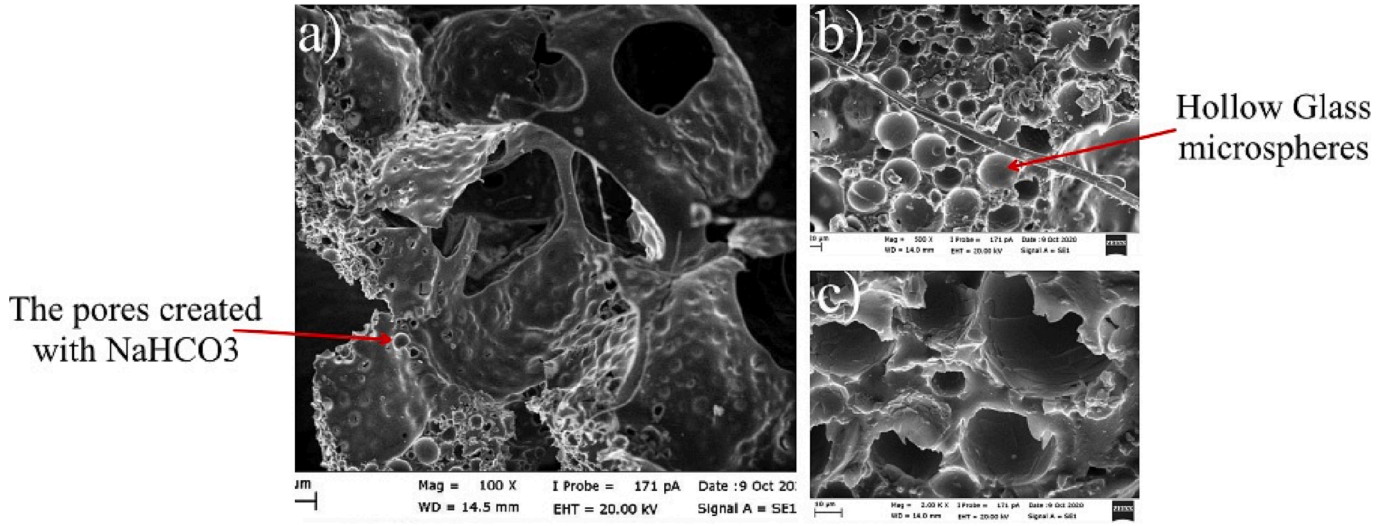

Fig. 5. SEM images of epoxy hybrid foam structures.

Table 1
The foam densities based on the wt% ratio of flexible epoxy, sodium bicarbonate, and hollow glass microspheres.

	Flexible Epoxy(A) + Hardener (B) wt%	$NaHCO_3$ wt%	Hollow Glass Microspheres wt%	Epoxy Foam Density (g/cm^3)
A	84	6	10	0.241
B	80	10	10	0.274
C	86	4	10	0.281
D	70	20	10	0.523
E	94	6	0	0.425

lightweight is essential, the use of excessive $NaHCO_3$ causes an increase in density. This value corresponds to the ratio of the respective molar masses of formed sodium carbonate Na_2CO_3 (106 g/mol) upon initial $NaHCO_3$ (168 g/mol) [46].

The homogeneous distribution of $NaHCO_3$ in the structure is significant. Agglomeration occurs when the use of $NaHCO_3$ exceeds specific rates. Sudden and severe pressure increases occur due to heat in the agglomerated regions. Thus, relatively large and monolithic cells emerge in a portion of the structure. In other parts, non-porous sections occur due to the low $NaHCO_3$ ratio. In this case, inhomogeneous density regions occur in the structure.

Specimen D showed that the foaming agent added at the rate of 20% caused large cells in the structure. In the remaining area, there was residual waste from the foaming agent. These wastes caused an increase in density in the specimen. Therefore, specimen D has a higher density. Sound waves choose the easy way and move towards big spaces.

3.2. Tensile and compression test results

This study used flexible epoxy to contribute to the refraction of sound waves. The flexible epoxy behavior (which does not contain HGMs and Sodium bicarbonate additives) under the tensile test is shown in Fig. 6. The experiment was carried out at a constant speed of 5 mm/min. It has

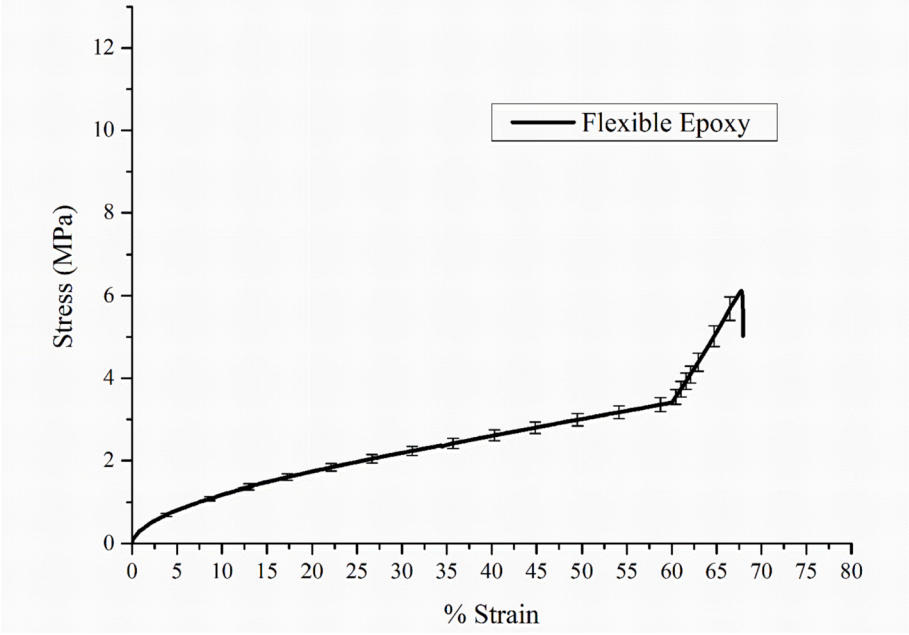

Fig. 6. Stress–strain curves of the flexible epoxy matrix material.

been observed that the developed sound insulation structure has superior tensile properties when compared to the polyurethane foams frequently used in the literature [47,48]. Thus, structures with more rigid and superior structural properties have been obtained against the loads on them.

HGMs were added to the flexible epoxy matrix as a filling material. The effect of this addition on the rigidity of the structure was investigated. In Fig. 7, the test specimen was subjected to a repeated compression test. The first experiment shows that the HGMs contribute to the structural strength and absorb 17.22 J of energy. The specimen is elastic. For this reason, when the load was removed, it quickly returned to its former form. During the experiment, the HGMs broke and lost their ability to absorb energy. The broken HGMs only served as filler in the repeated compression test on the same specimen. As a result, 9.8 J energy absorption occurred in the structure. Compression tests were repeated after the first tests on the flexible epoxy specimen without HGMs to determine whether the structure was damaged and the energy absorption decreased. The curves obtained from the pure epoxy compression test are similar to those in the 2nd experiment. The absorbed energy obtained from this test is 9.45 Joules. As can be seen from the results, damage to HGMs caused a significant decrease in energy absorption.

The samples obtained by filling foams of different densities into the Al honeycomb core cells were subjected to the compression test (Fig. 8). In addition, the empty Al honeycomb was tested and compared in order to see the contribution of the foam filling to the Al honeycomb cell walls under compression loading. In the experiment, it is observed that the foam filling increases the bending rigidity and also critical buckling load of the honeycomb cell walls by supporting them from the inside. In particular, high reaction forces were observed in the sandwich structure filled with high-density foam. As the force on the specimens caused the initial damage to the Al walls, plateau zones occurred in the curves. After specific displacements, the folding of the honeycomb cell walls ended, and the reaction force increased. These displacements were not observed in high-density specimens because the filled foam deformation capacity was smaller than the others.

The areas under the stress–strain curves shown in Fig. 9 demonstrate the energy absorbed. The force on the structure releases energy along with the deformation. In this context, both stress and strain are desired to be high. Although the strain of the empty sandwich structure is high, the reaction force is low. The cell strength of the honeycomb walls increased with foam fillings of different densities. Thus, high-stress values were obtained. With the increase of foam filling densities, the deformation capacity of the walls decreased. Therefore, a decrease in the amount of deformation is observed. Thus, lower strain values were obtained. The area under the curves given in Fig. 9 was calculated by the multiple integration methods (Equation (6)) [49].

$$I = \int_c^d \int_a^b f(x,y)dxdy \cong \int_c^d \left(\sum_{i=1}^{n} f(x_i,y).\Delta x\right)dy = \int_c^d g(y)dy = \\ = \sum_{j=1}^{m} g(y_j).\Delta y \tag{6}$$

When Fig. 9 is examined, the energy absorption value of the empty Al honeycombs is 31.75 J, and the energy absorption values of the foam-filled structures increased approximately 1.5 times with the increasing density.

3.3. Three-Point bending test

The developed sound insulation material was an elastic foam. Therefore, this material has low bending stiffness. For use in structural applications as much as thermal insulation and sound absorption, It has benefited as a filler in the Al honeycomb sandwich core structure. Thus, structural integrity was also preserved. During the three-point bending test, the sandwich structure is under concentrated load between two simple supports, producing bending moment and shear force. When a honeycomb core is filled with foam, the honeycomb core cell walls' bending rigidity and critical buckling load increase. Hence, these sandwich structures performed higher compression loads resistivity. When the empty honeycomb core sandwich specimen was subjected to a three-point bending test, the Al honeycomb cell walls could not resist bending and buckling more in the local region around the loading point (Fig. 10). Hence, the honeycomb cell walls started wrinkling and folding around this region. And then it was followed by the local core crush.

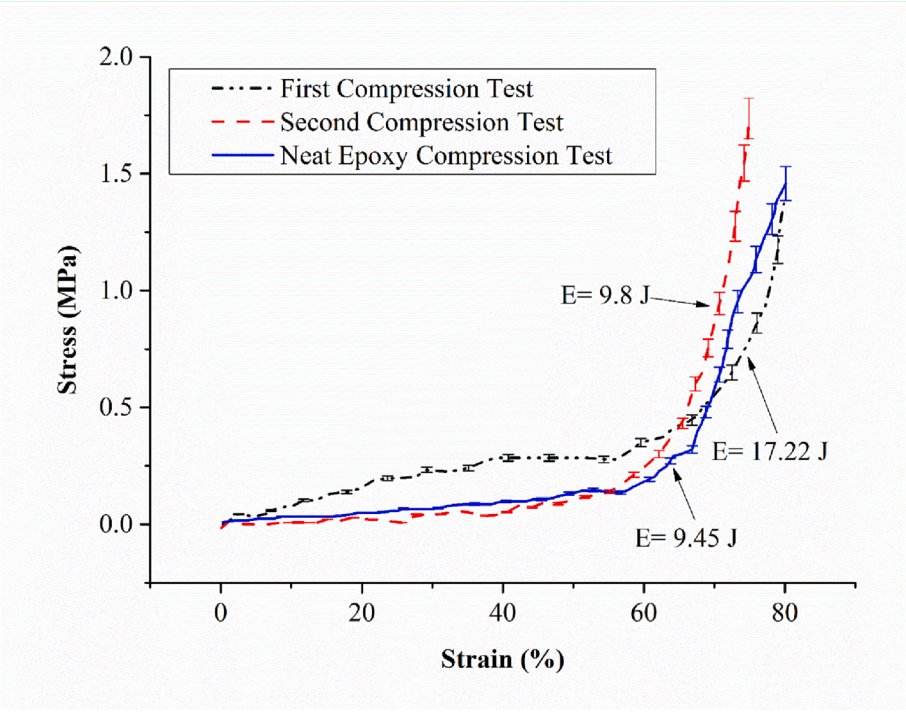

Fig 7. The stress–strain curve of the foam material.

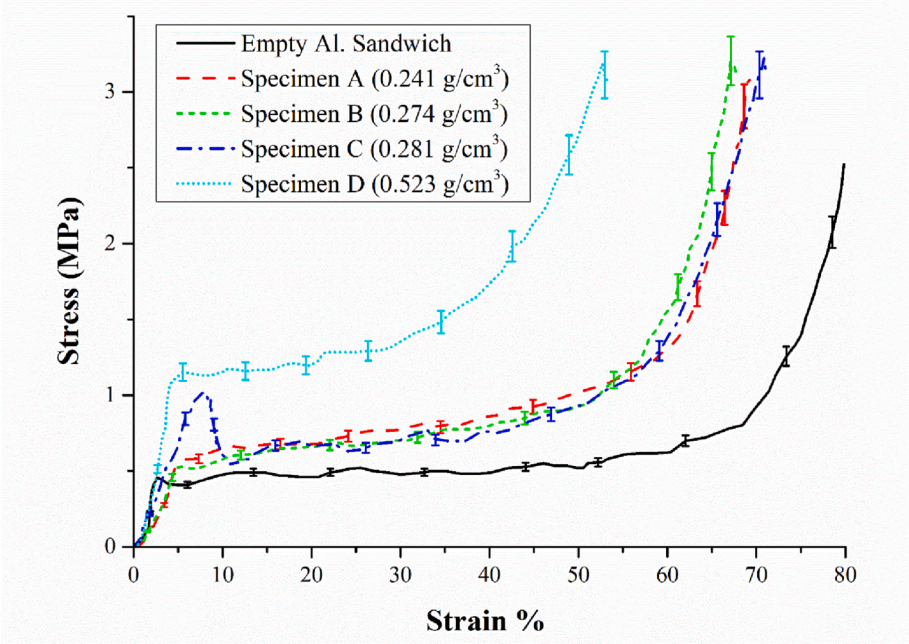

Fig. 8. The compression strength of epoxy foam specimens in different densities.

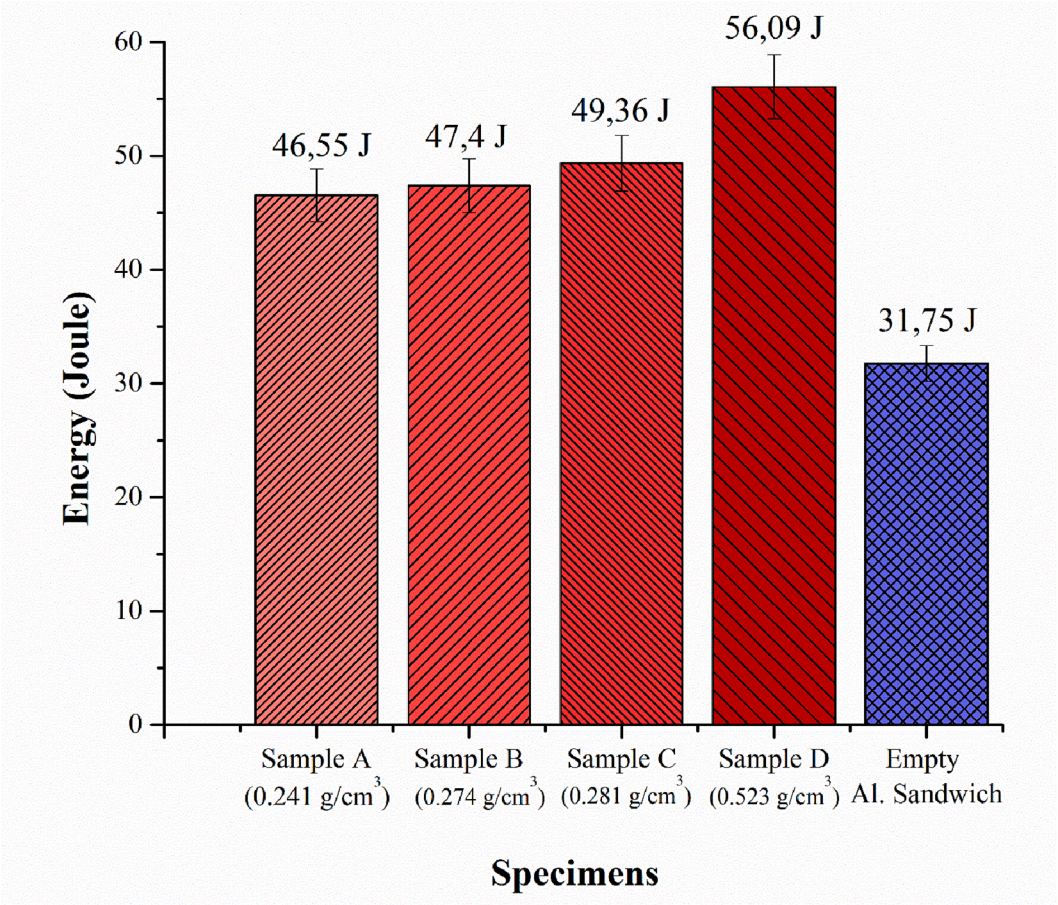

Fig. 9. Comparison of energy absorption values of sandwich specimens produced.

Then, a plastic hinge occurred at this point of the sandwich beam, and a rotational motion was started around this point. In this stage, the sandwich beam showed less bending moment resistivity. As a result of this behavior, the applied load dropped dramatically right after reaching the maximum force of 1150 N. Then, it continues to deform under the force of approximately 400 N. During this time, 28.2 J of energy was

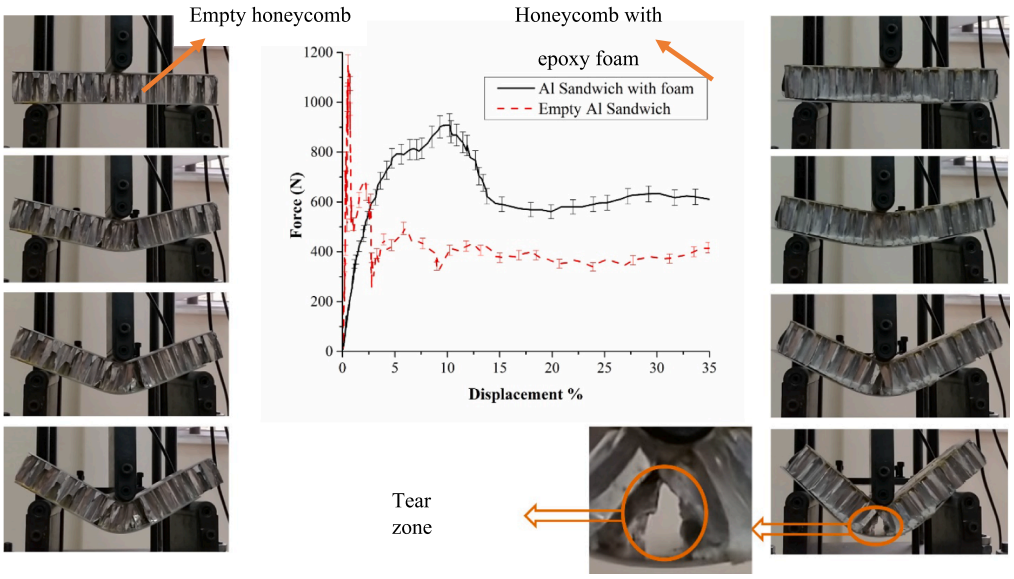

Fig. 10. Force-displacement curves of three-point bending test.

absorbed. In the foam-filled sandwich specimen, the cell walls of the Al honeycomb become more resistant to bending and buckling under the loading point region. As a result, the bending load on the supported cell walls is transmitted to the bottom face of the structure as a form of tensile load without transforming into local deformation. Hence, the plastic hinge, in this case, occurred at the loading point on the top face sheet. So, bending the moment was transferred as a tensile load to the bottom face. Around 1000 N, the Al bottom face sheet started to elongate plastically. Because the foam-filled Al honeycomb core could not follow this extension, crushing strength increased with the foam filling, and the core started tearing from the bottom face interface. As a result of this behavior, the amount of energy absorbed was determined as 45.1 J.

3.4. Sound insulation sound and transmission

The loss of sound transmission could be expressed as the sum of absorbed and projected sound. Fig. 11 shows the sound transmission loss (STL) values of the aluminum sandwich structures filled with flexible epoxy in four different densities. It was seen that the STL value of the aluminum honeycomb without foam filling was the lowest. The lowest-density foam-filled sandwich specimen achieved the highest sound transmission loss value. At higher frequencies, it is seen that foam density and sound transmission loss are inversely proportional.

Fig. 12 was given sound absorption coefficients depending on the increased frequency. The empty aluminum honeycomb structure does not affect the absorption of sound waves at low frequencies. When the frequency of the sound waves increases, the waves reflected from the aluminum walls cause refraction of the incoming waves. Because high reverberation occurs in aluminum walls, therefore, it was observed that the sound absorption coefficient increased at high frequencies. When the sound absorption coefficients of the foam-filled sandwich specimens of different densities were examined, it was seen that the low-density specimens reached higher sound absorption values at low frequencies. With the increase in sandwich density, superior sound absorption was achieved at higher frequencies.

The superior sound absorption frequency values of specimens with

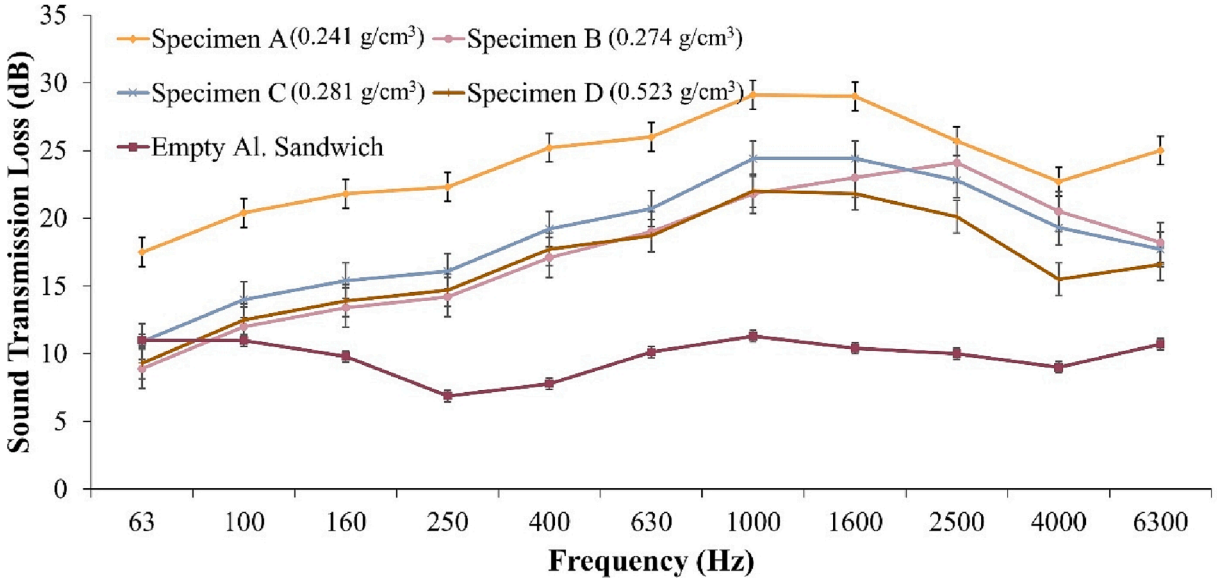

Fig. 11. Created sandwich specimens sound transmission loss-frequency graph.

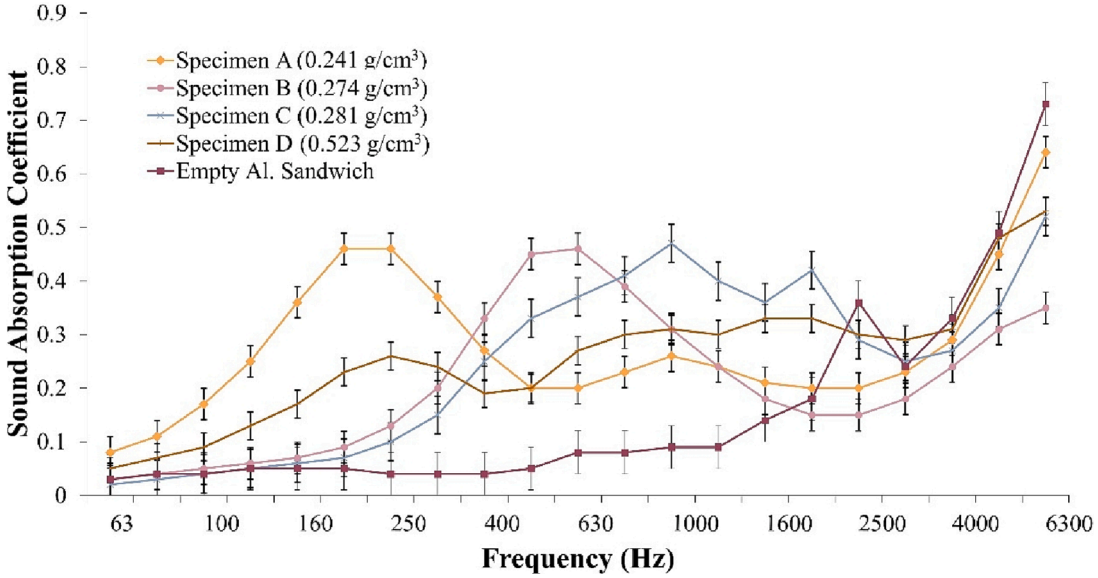

Fig. 12. Sound absorption coefficients of specimens in different densities.

different densities are shown in Fig. 13. While A specimen had superior absorption at 150–350 frequency values, B specimen could be used as sound-absorbing material at 350–950 frequency values. C and D specimens, on the other hand, showed superior sound absorption performance at higher frequencies.

The study investigated the contribution of HGM to the sandwich structure sound transmission loss and sound absorption coefficient. Sound transmission coefficient and sound absorption values of A specimens containing 6% $NaHCO_3$ and 10% HGM and E specimens containing only 6% $NaHCO_3$ were compared.

While large cells are formed with the contribution of $NaHCO_3$, low-density HGMs perform a filling function in the matrix material. Thus, specimens with lower density are obtained. Some sound waves from the HGMs contributing to the decrease in density are refracted and imprisoned in the HGMs. In addition, HGMs allow the reflection of sound waves. Thus, a high sound absorption coefficient is obtained at low frequencies. It is known that high-density (thick and solid) structures exhibit superior performance at increasing frequency values. In Fig. 14, an increase in the sound absorption coefficient of high-density specimens was observed after the frequency values of about 500 Hz.

In Fig. 15, a significant increase was observed in the sound transmission loss values of the A specimen with HGM added. Because when the sound waves come into contact with the HGM walls in the matrix, reflections, and refractions occur. Thus, the waves are weakened and trapped in the closed microsphere pores.

3.5. DSC and TGA Analyze

When the DSC graph of the epoxy foam with optimum sound absorption was examined, 3 peaks were observed. The decomposition temperature of the residual sodium bicarbonate is 93.6 °C (Fig. 16). The peak of the polyether-based amine used in curing the cross-linked epoxy foam is at 135.4 °C, and the peak at 172.9 °C is the bisphenol-A-based temperature epoxy main chain can move [50,51].

When the TGA thermogram of the sample with the best sound absorption was examined, the first mass loss occurred at around 100 °C. It is estimated that this loss will be caused by the water and solvent contained in the structure. 5% mass loss occurs at 260 °C, which is quite good compared to other vinyl polymers. The sample lost 69% of its mass between 380 and 420 °C, which is quite good at this value. At 800 °C,

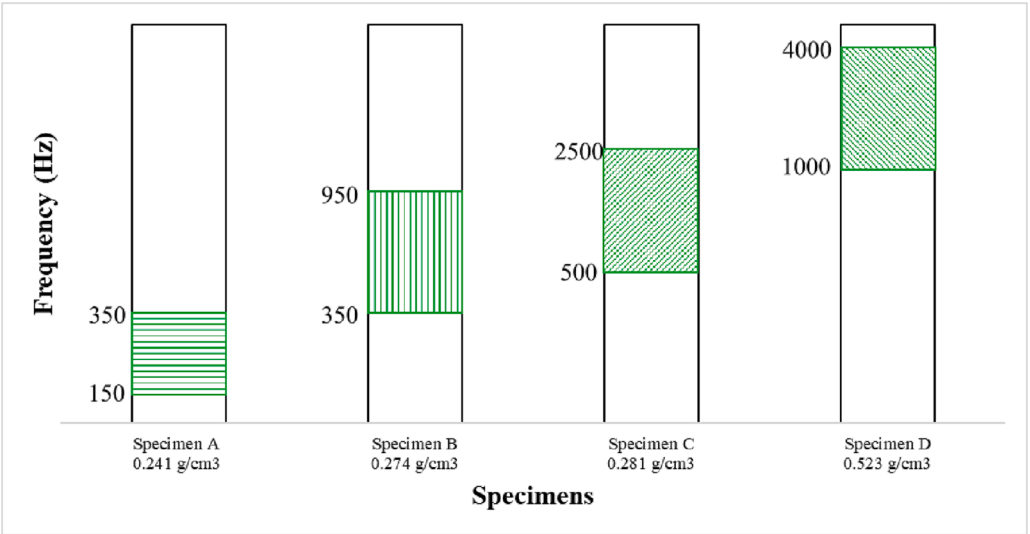

Fig. 13. Superior absorption frequencies vary depending on the density.

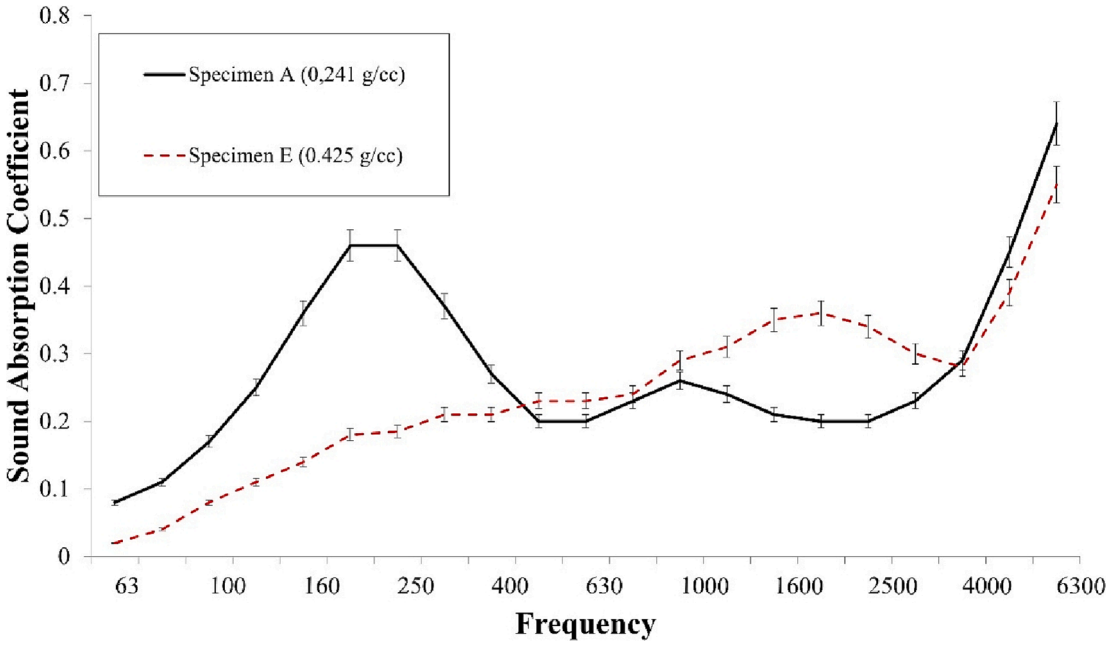

Fig. 14. Effect of HGM on the sound absorption coefficient.

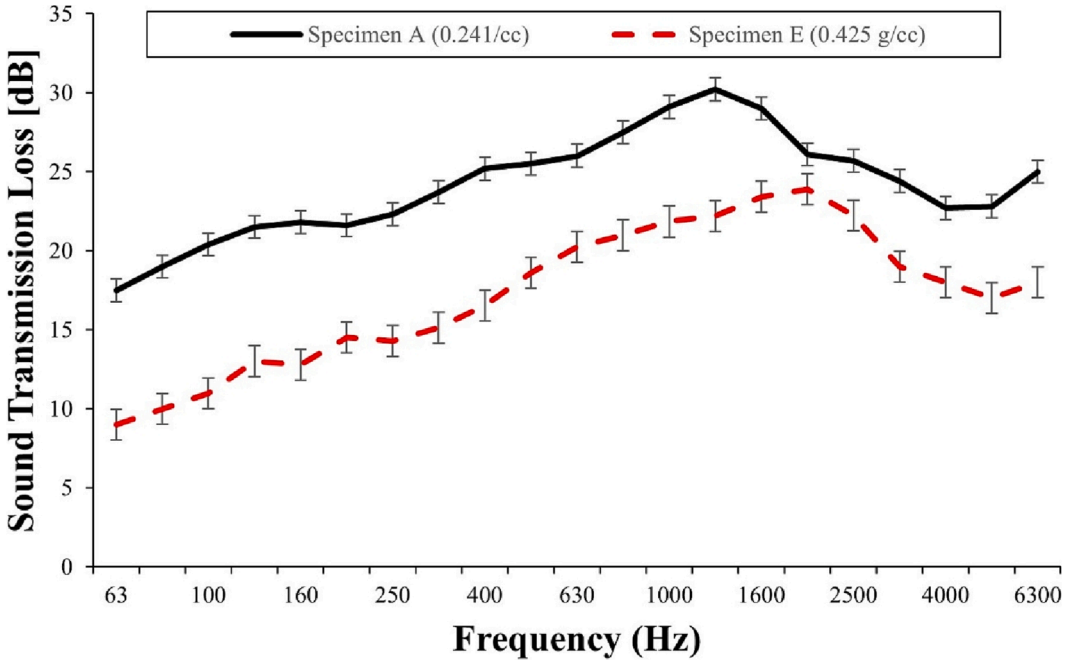

Fig. 15. Effect of HGM on sound transmission loss.

quite a lot of residue remains compared to a polymer. This high amount of residue is thought to be due to sodium carbonate. (Fig. 17)

3.6. Dielectric test

The dielectric properties apply to insulating materials used in different fields and operating conditions [52]. Dielectric constant (ϵ) and loss factor (tanδ) are essential in these properties. The dielectric constant of the insulator changes with frequency (F) and temperature (T). As the frequency increases, the dielectric constant decreases [53].

A dielectric measurement specimen was produced using the optimal sound absorption hybrid foam. The dielectric constant for the specimen tested was measured as 10,187 at 10 kHz at room temperature (Fig. 18).

The dielectric loss is caused by failure to follow the rate of change of electricity applied to the polarization process in a molecule. This situation is due to the polymer's relaxation period (τ), which is taken to return to the original random orientation. The relaxation period is smaller than the released electric field's speed, so the dielectric loss is not lost at a minimum. In our study, there was a sharp decline observed at the point of about 10 kHz. The loss factor for the specimen tested was measured as 0.37% at 10 kHz at room temperature (Fig. 19). The loss factor was desired to be minimum when choosing the insulation material. Insulating material energy loss occurs when electrical energy is applied to them. The voltage-current angle is below 90°. Besides, the tangent value of the dielectric loss (tanφ) is supplied Sin(90-φ) equality.

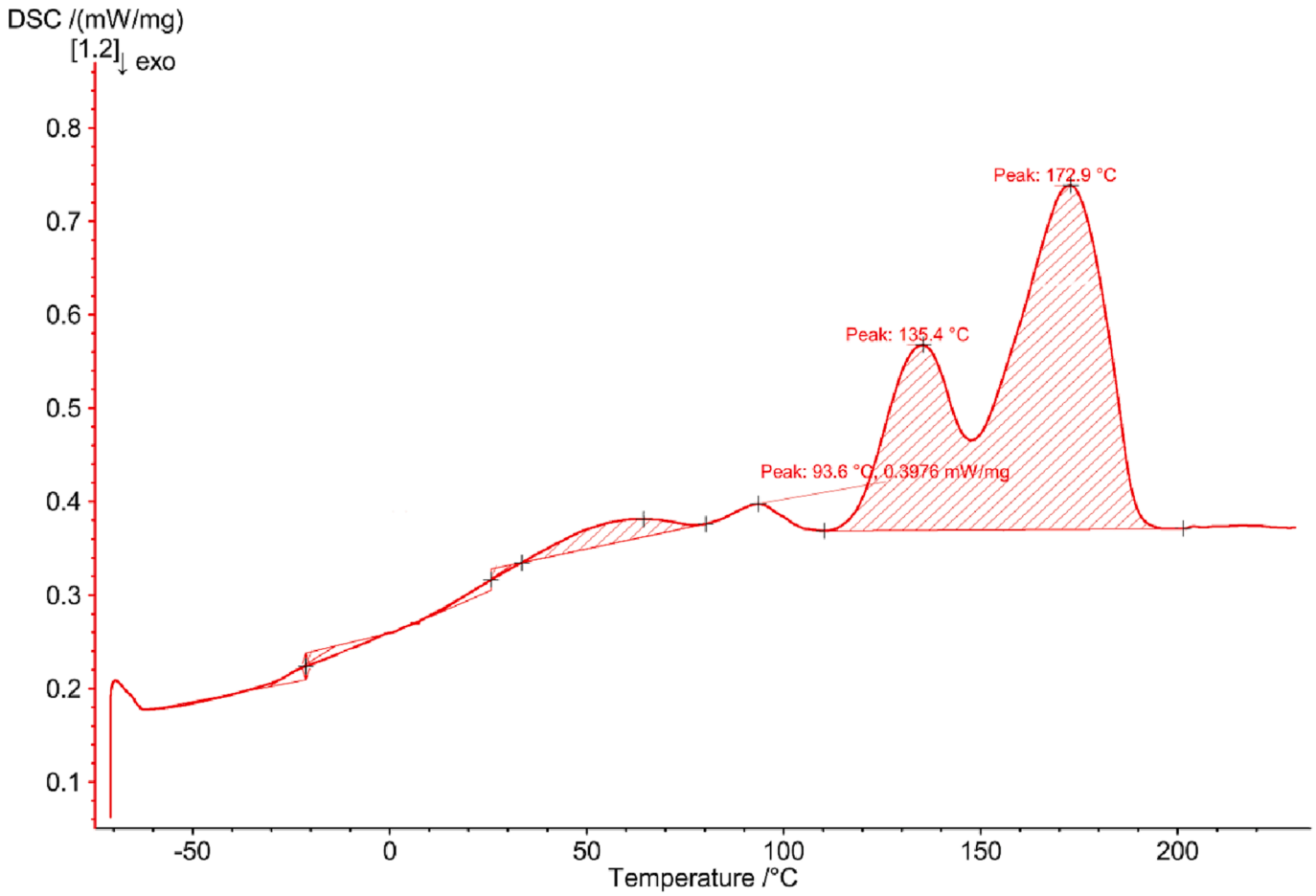

Fig. 16. Epoxy foam DSC diagram.

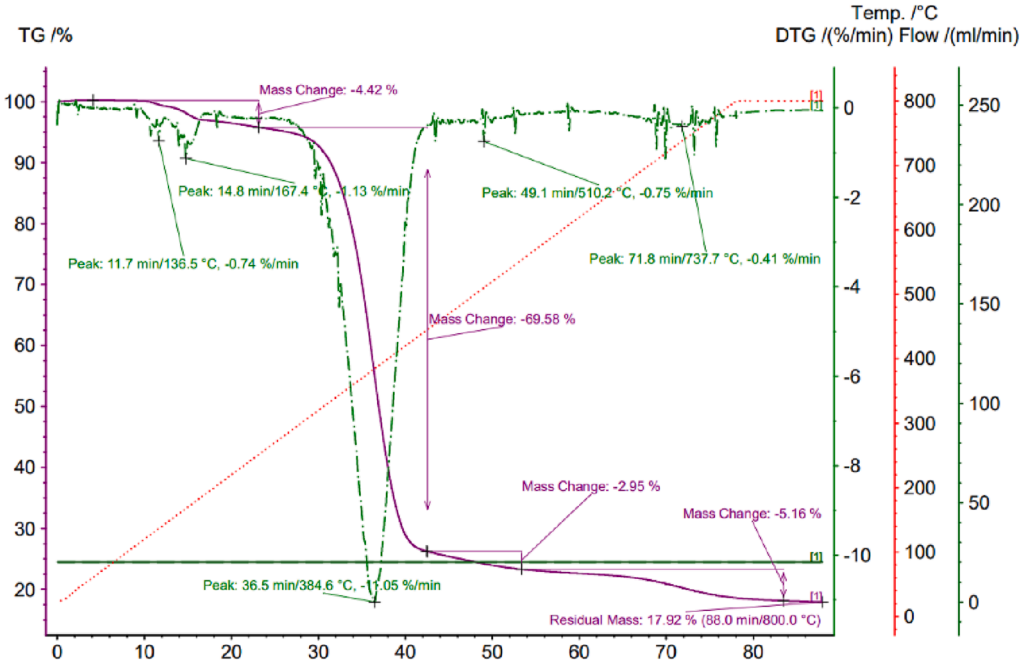

Fig. 17. TGA curve of the epoxy foam specimen developed.

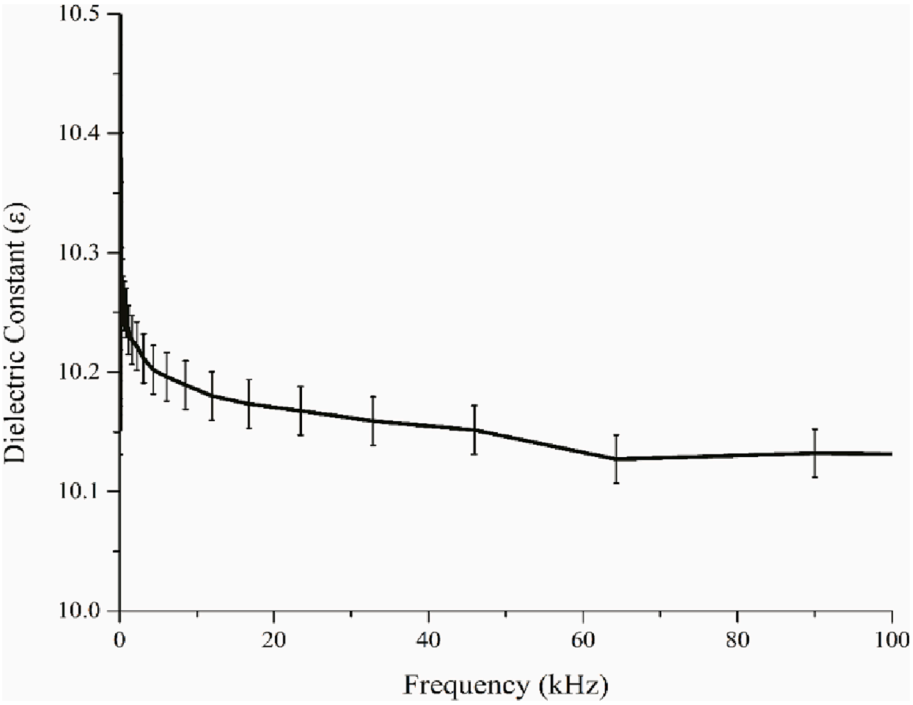

Fig. 18. The dielectric constant of hybrid epoxy specimen - frequency change.

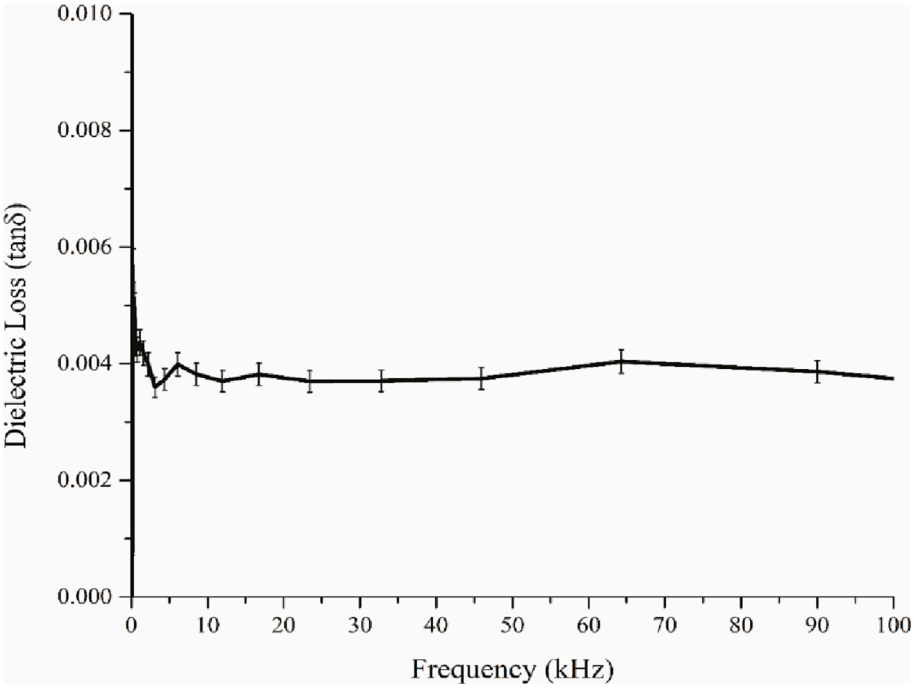

Fig. 19. The dielectric loss of hybrid epoxy foam specimen - frequency change.

3.7. Thermal conductivity test

Thermal conductivity is the most crucial thermophysical property used to describe the heat transfer properties of materials. The thermal conductivity coefficient λ is defined as the energy transfer rate across the unit area of the surface when dT/dy is a unit temperature gradient perpendicular to the surface. It is measured utilizing the International Systems of Unit (SI unit) of W/m•K. This coefficient is complementary to thermal resistivity, which measures the capacity of an object to stand up to thermal exchange. [54]

The specimens to be tested have a minimum thickness of 50 mm and a diameter of 30 mm. A suitable smooth surface of the material to be measured is contacted with the device's sensor. Thus, the device determines the material's thermal conductivity coefficient (k) in W/mK based on the temperature interaction between the sensor and specimen. This test was conducted at room temperature, and three measurements were made for testing. The thermal conductivity coefficient was calculated by taking the average of these three measurements.

The thermal conductivity analysis results show that the average thermal conductivity coefficient is 0.064 (W/mK). Thermal insulation materials defined in European Standards have a thermal conductivity coefficient below $\lambda = 0.065$ W/mK. Therefore, the syntactic foam with a flexible epoxy matrix produced in our study is considered a thermal insulation material [55].

3.8. Flammability

This research is not directly focused on non-flammability. UL 94 HBF tests were conducted anyway. In accordance with the results of the flammability test for the UL 94 HBF class, specimen D (0.52 g per cubic centimeter) was entirely burned by fire within 10 s. When HGMs are added to an epoxy matrix, the results are consistent with the published literature [55]. Incorporating fire-resistant materials can reduce flammability rates. For example, when aluminum di-isobutyl-phosphinate was added to the epoxy syntactic foam, which is formed by mixing epoxy matrix with HGMs, Xiang et al. [56] obtained V-1 flame retardancy without dripping. This demonstrates that vertical surfaces can stop burning within 30 s.

4. Conclusion

In this study, cellular flexible epoxy matrix sound-absorbing materials with different densities were developed. The epoxy matrix was mixed with HGMs and blowing agents. During the foaming of the epoxy resin, all HGMs were relocated to the cell walls of the foam. This shape enhanced the acoustic absorption properties of the flexible epoxy foam. Thus, the sound waves will be broken, dissipated, and reflected when passing through the epoxy foam cell walls, much more. Compression tests were performed to obtain this hybrid syntactic epoxy foam load-carrying capacity. The contribution to the bending resistance of the foam filler was examined with three-point bending tests. The flexible epoxy matrix syntactic foam specimen thermal and electrical characterizations were made. The following conclusions have been accessed as a result of the experimental studies.

1) A novel foam was developed in the study, formed by large cells, their cell walls having rigid HGMs inclusions for superior acoustic performance.
2) Sound absorption coefficients of 0–6300 frequency values of the developed structure with different densities were examined. It has been observed that low-density structures exhibit superior performance at low frequencies and high-density structures at high frequencies. It is known that hybrid and electric vehicles cause vibration and noise in a broader frequency range than internal combustion engines. It is foreseen that the developed structure can be used as a sound-dampening element in the engine blocks of new-generation electric cars or other electric vehicles. In the sound transmission loss tests performed by adding HGM to increase the sound transmission loss, it is seen that the HGMs break the sound waves and trap them in their closed pores.
3) The sandwich structure's energy absorption performance is enhanced by foam filling. Thus, it has been determined that the developed structure provides rigidity to the honeycomb cell walls as well as sound insulation. In addition to aiding in sound absorption as a filler, the stiffness of HGMs also increased flexible epoxy foam compression load-bearing capacity.
4) In case an empty honeycomb core sandwich specimen has low core compression resistivity, a local core crush occurs at the loading point. At this point, a plastic hinge occurred a rotational motion started around this point. In this stage, the sandwich beam performed less bending moment resistivity. The subjected load decreased dramatically at this time.
5) In the foam-filled sandwich specimen, the plastic hinge occurred on the loading point due to the high crush resistivity and more tensile load transferred to the bottom face sheet, causing it to elongate plastically. Because the foam-filled Al honeycomb core could not follow this extension, foam filled core tore starting bottom face midpoint.
6) Another energy absorption mechanism, such as the core tearing, appeared in the foam-filled Al honeycomb sandwich specimen.
7) In the DSC and TGA analyses performed for epoxy foam, sodium bicarbonate and HGMs in the foam were observed. The degradation temperatures of sodium bicarbonate were clearly observed in the DSC thermogram. In addition, the mass residues observed as 17.92% of the epoxy foam at 800°in TGA analysis belong to HMS and degradation residues of sodium bicarbonate.
8) It is determined that this material shows the insulating property when the dielectric feature of the flexible epoxy matrix syntactic foam specimen of optimum sound absorption is evaluated. Especially it is thought to be a precaution against possible electrical leakages and improve the acoustic performance of electric motors.
9) The thermal conductivity coefficient of the flexible epoxy matrix syntactic foam specimen is under the value of $\lambda = 0.065$ w / mK, so this material showed a superior thermal insulation property. It is essential that electric motors with long operating times are protected from thermal environmental factors and that the heated electric motor does not affect the outside temperature.
10) Developed syntactic foams are not non-flammable material in the current combination. However, the production technique of the epoxy syntactic foam is suitable for contributing flame retardant materials as an additive inside the composite to get non-flammable material.

CRediT authorship contribution statement

Yalçın Boztoprak: Conceptualization, Methodology, Writing – review & editing. **Merve Ünal:** Investigation, Writing – original draft. **Çağatay Özada:** Investigation, Writing – original draft. **Eslem Kuzu:** Investigation, Writing – original draft. **Hakkı Özer:** Investigation, Writing – original draft. **Furkan Ergin:** Investigation, Writing – original draft. **Murat Yazıcı:** Conceptualization, Methodology, Writing – review & editing, Project administration, Funding acquisition, Supervision.

Declaration of Competing Interest

The authors declare that they have no known competing financial interests or personal relationships that could have appeared to influence the work reported in this paper.

Data availability

No data was used for the research described in the article.

Acknowledgements

The authors would like to thank the Scientific and Technological Research Council of Turkey (Tübitak) for their support through Project Number 218 M468. Co-authors Çağatay ÖZADA and Merve ÜNAL are supported by YÖK 100/2000 as scholarship holders in the priority field of "Smart and innovative materials" In addition, co-authors Çağatay ÖZADA is a Ph.D. scholar in TÜBİTAK 2211/C Priority areas. The authors would also like to thank PECHOM Co./Bursa/Türkiye for their help with acoustic measurements.

References

[1] Cao L, Fu Q, Si Y, Ding B, Yu J. Porous materials for sound absorption. Compos Commun 2018. https://doi.org/10.1016/j.coco.2018.05.001.

[2] Organization WH. Burden of disease from environmental noise: Quantification of healthy life years lost in Europe. Regional Office for Europe: World Health Organization; 2011.
[3] Chua JW, Li X, Yu X, Zhai W. Novel slow-sound lattice absorbers based on the sonic black hole. Compos Struct 2023;304:116434. https://doi.org/10.1016/j.compstruct.2022.116434.
[4] Cobo P, Montero de Espinosa F. Proposal of cheap microperforated panel absorbers manufactured by infiltration. Appl Acoust 2013;74:1069–75. https://doi.org/10.1016/J.APACOUST.2013.03.003.
[5] Arenas JP, Ugarte F. A note on a circular panel sound absorber with an elastic boundary condition. Appl Acoust 2016;114:10–7. https://doi.org/10.1016/J.APACOUST.2016.07.002.
[6] Arenas JP, Crocker MJ. Recent Trends in Porous Sound-Absorbing Materials. Sound Vib 2010;44:12–8.
[7] Bardakhanov SP, Lee C-M, Goverdovskiy VN, Zavjalov AP, Zobov KV, Chen M, et al. Hybrid sound-absorbing foam materials with nanostructured grit-impregnated pores. Appl Acoust 2018;139:69–74. https://doi.org/10.1016/j.apacoust.2018.04.024.
[8] Berardi U, Iannace G. Acoustic characterization of natural fibers for sound absorption applications. Build Environ 2015;94:840–52. https://doi.org/10.1016/j.buildenv.2015.05.029.
[9] Xinzhao X, Guoming L, Dongyan L, Guoxin S, Rui Y. Electrically conductive graphene-coated polyurethane foam and its epoxy composites. Compos Commun 2018;7:1–6.
[10] Álvarez-Láinez M, Rodríguez-Pérez MA, De Saja JA. Acoustic absorption coefficient of open-cell polyolefin-based foams. Mater Lett 2014;121:26–30. https://doi.org/10.1016/j.matlet.2014.01.061.
[11] Notario B, Ballesteros A, Pinto J, Rodríguez-Pérez MA. Nanoporous PMMA: A novel system with different acoustic properties. Mater Lett 2016;168:76–9. https://doi.org/10.1016/j.matlet.2016.01.037.
[12] Xue B, Deng J, Zhang J. Multiporous open-cell poly(vinyl formal) foams for sound absorption. RSC Adv 2016;6:7653–60. https://doi.org/10.1039/c5ra23285f.
[13] Xu Y, Li Y, Zhang A, Bao J. Epoxy foams with tunable acoustic absorption behavior. Mater Lett 2017. https://doi.org/10.1016/j.matlet.2017.02.054.
[14] Wenbo ZHU, Shuming C, Yebin W, Tongtong ZHU, Jiang Y. Sound absorption behavior of polyurethane foam composites with different ethylene propylene diene monomer particles. Arch Acoust 2018;43:403–11.
[15] Pirani M, Monazzam MR, Pourjandaghi SQ. Correlation Between the Acoustic and Cell Morphology of Polyurethane/Silica Nanocomposite Foams: Effect of Various Proportions of Silica at Low Frequency Region. J Heal Saf Work 2021;11:1–12.
[16] Gupta N, Priya S, Islam R, Ricci W. Characterization of mechanical and electrical properties of epoxy-glass microballoon syntactic composites. Ferroelectrics 2006;345:1–12. https://doi.org/10.1080/00150190601018002.
[17] Park S-J, Jin F-L, Lee C. Preparation and physical properties of hollow glass microspheres-reinforced epoxy matrix resins. Mater Sci Eng A 2005;402:335–40. https://doi.org/10.1016/j.msea.2005.05.015.
[18] Ding J, Liu Q, Ye F, Zhang H, Gao Y, Zhang B. Compressive properties of co-continuous hollow glass microsphere/epoxy resin syntactic foams prepared using resin transfer molding. J Reinf Plast Compos 2019;39:132–43. https://doi.org/10.1177/0731684419877568.
[19] Gao G, Hu Y, Jia H, Liu P, Du P, Xu D. Acoustic and dielectric properties of epoxy resin/hollow glass microsphere composite acoustic materials. J Phys Chem Solids 2019;135:109105. https://doi.org/10.1016/j.jpcs.2019.109105.
[20] Özer H, Can Y, Yazici M. Investigation of the crash boxes Light weighting with syntactic foams by the finite element analysis. Acta Phys Pol A 2017;132:734–7. https://doi.org/10.12693/APhysPolA.132.734.
[21] Hu G, Yu D. Tensile, thermal and dynamic mechanical properties of hollow polymer particle-filled epoxy syntactic foam. Mater Sci Eng A 2011;528:5177–83. https://doi.org/10.1016/j.msea.2011.03.071.
[22] van Belle B. Advances in High-Temperature Syntactic Foam Technology for Offshore Systems. Offshore Technol Conf 2002:6. https://doi.org/10.4043/14120-MS.
[23] Anirudh S, Jayalakshmi CG, Anand A, Kandasubramanian B, Ismail SO. Epoxy/glass syntactic foams for structural and functional application-A review. Eur Polym J 2022;111163.
[24] Zhang Z, Jiang H, Li R, Gao S, Wang Q, Wang G, et al. High-damping polyurethane/hollow glass microspheres sound insulation materials: Preparation and characterization. J Appl Polym Sci 2021;138:1–10. https://doi.org/10.1002/app.49970.
[25] Cosse RL, Araujo FH, Pinto FA, de Carvalho LH, de Morais ACL, Barbosa R, et al. Effects of the type of processing on thermal, morphological and acoustic properties of syntactic foams. Compos B Eng 2019;173:106933.
[26] Chen Z, Qin Y, Huang ZX, Shen Q, Zhang LM. Preparation and characterization of novel functional gradient syntactic foam. In Advanced Materials Research 2009;2009(66):284–7.
[27] Demir E, Güler Ö. Production and properties of epoxy matrix composite reinforced with hollow silica nanospheres (HSN): mechanical, thermal insulation, and sound insulation properties. J Polym Res 2022;29:477.
[28] Sennewald C, Kaina S, Weck D, Gruhl A, Thieme M, Hoffmann G, et al. Metal sandwiches and metal-matrix-composites based on 3D woven wire structures for hybrid lightweight construction. Adv Eng Mater 2014;16:1234–42.
[29] Sun Y, Guo L cheng, Wang T shu, Zhong S yang, Pan H zhu. Bending behavior of composite sandwich structures with graded corrugated truss cores. Compos Struct 2018. https://doi.org/10.1016/j.compstruct.2017.11.043.
[30] Birman V, Kardomateas GA. Review of current trends in research and applications of sandwich structures. Compos Part B Eng 2018. https://doi.org/10.1016/j.compositesb.2018.01.027.
[31] Wang B, Yang M. Damping of honeycomb sandwich beams. J Mater Process Technol 2000;105:67–72. https://doi.org/10.1016/S0924-0136(00)00564-1.
[32] Maheri MR, Adams RD. Steady-state flexural vibration damping of honeycomb sandwich beams. Compos Sci Technol 1994;52:333–47. https://doi.org/10.1016/0266-3538(94)90168-6.
[33] Naify C, Sneddon M, Nutt S. Noise reduction of honeycomb sandwich panels with acoustic mesh caps. Proc Meet Acoust 2010;8. https://doi.org/10.1121/1.3274775.
[34] Sui N, Yan X, Huang TY, Xu J, Yuan FG, Jing Y. A lightweight yet sound-proof honeycomb acoustic metamaterial. Appl Phys Lett 2015;106:1–5. https://doi.org/10.1063/1.4919235.
[35] Griese D, Summers JD, Thompson L. The effect of honeycomb core geometry on the sound transmission performance of sandwich panels. J Vib Acoust Trans ASME 2015;137:1–11. https://doi.org/10.1115/1.4029043.
[36] Assaf S, Guerich M. Numerical prediction of noise transmission loss through viscoelastically damped sandwich plates. J Sandw Struct Mater 2008;10:359–84. https://doi.org/10.1177/1099636207088444.
[37] Keener TC, Frazier GC, Davis WT. Thermal decomposition of sodium bicarbonate. Chem Eng Commun 1985;33(1–4):93–105.
[38] Babushok VI, McNesby KL, Miziolek AW, Skaggs RR. Modeling of synergistic effects in flame inhibition by 2-H heptafluoropropane blended with sodium bicarbonate. Combust Flame 2003;133:201–5. https://doi.org/10.1016/S0010-2180(02)00572-2.
[39] Standard A. C384-04,". Stand Test Method Impedance Absorpt Acoust Mater by Impedance Tube Method", ASTM Int West Conshohocken, PA, USA 2004.
[40] Fahy F. Foundations of Engineering Acoustics. Elsevier Ltd 2003. https://doi.org/10.1016/B978-0-12-247665-5.X5000-0.
[41] Can Y. Sound insulation performance of short cotton fibre waste/recycled acrylonitrile butadiene styrene composites. Acta Phys Pol A 2019;135:772–4. https://doi.org/10.12693/APhysPolA.135.772.
[42] Shechter L, Wynstra J. Glycidyl Ether Reactions with Alcohols, Phenols, Carboxylic Acids, and Acid Anhydrides. Ind Eng Chem 1956;48:86–93. https://doi.org/10.1021/ie50553a028.
[43] Matejka L, Pokorny SDK. Network formation involving epoxide and carboxyl groups - course of the model reaction monoepoxide-monocarbonic acid. Polym Bull 1980;440:437–40.
[44] Blank W, He Z. Catalysis of the Epoxy-Carboxyl Reaction. Int Waterborne, High-Solids 2001;74:33–41.
[45] Supanchaiyamat N, Shuttleworth PS, Hunt AJ, Clark JH, Matharu AS. Thermosetting resin based on epoxidised linseed oil and bio-derived crosslinker. Green Chem 2012;14:1759–65. https://doi.org/10.1039/c2gc35154d.
[46] Mazzon E, Habas-Ulloa A, Habas JP. Lightweight rigid foams from highly reactive epoxy resins derived from vegetable oil for automotive applications. Eur Polym J 2015;68:546–57. https://doi.org/10.1016/j.eurpolymj.2015.03.064.
[47] Kiddell S, Kazemi Y, Sorken J, Naguib H. Influence of Flash Graphene on the acoustic, thermal, and mechanical performance of flexible polyurethane foam. Polym Test 2023;107919.
[48] Ridha M, Shim VPW. Microstructure and tensile mechanical properties of anisotropic rigid polyurethane foam. Exp Mech 2008;48:763–76.
[49] Larson R, Edwards B. Multivariable Calculus. 10th Ed. Liz Covello; n.d.
[50] Calafel MI, Remiro PM, Cortázar MM, Calahorra ME. Cold crystallization and multiple melting behavior of poly(L-lactide) in homogeneous and in multiphasic epoxy blends. Colloid Polym Sci 2010;288:283–96. https://doi.org/10.1007/s00396-009-2156-3.
[51] Yao SJ, Zhou ZF, Ye F, Tian Z, Wang SM. Modifying sodium bicarbonate for foaming polymers. Adv. Mater. Res., vol. 940, Trans Tech Publ; 2014, p. 59–62.
[52] İnal M, Aras F. Determination of dielectric properties of insulating materials using artificial neural networks. J Fac Eng Archit Gazi Univ 2005;20:455–62.
[53] Hummel RE. Electronic properties of materials, vol. 3. Springer; 2011.
[54] Parsonage NG. Chapter 6- Thermal Conductivity. In: Parsonage NG, editor. The Gaseous State, Pergamon; 1966, p. 83–92. https://doi.org/https://doi.org/10.1016/B978-0-08-011867-3.50013-1.
[55] Xiang Y, Wang L, Yang Z, Gao P, Qin S, Yu J. Effect of aluminum phosphinate on the flame-retardant properties of epoxy syntactic foams. J Therm Anal Calorim 2019;137:1645–56.